Extraction of Nonlinear Waveforms in Geodesic Acoustic Modes by using Conditional Average

Kazutaka OZAWA¹⁾, Makoto SASAKI^{1)*}, Yohei HARA¹⁾, Tatsuya KOBAYASHI²⁾

¹⁾ Collage of Industrial Technology, Nihon University, Narashino 275-8575, Japan ²⁾ National Institute for Fusion Science, National Institutes of Natural Sciences, Toki 509-5292, Japan

(Received 27 May 2025 / Accepted 29 July 2025)

In L-mode plasmas of the JFT-2M tokamak, we applied conditional averaging to time-series data of electrostatic potential fluctuations measured by the Heavy Ion Beam Probe (HIBP). The analyzed phase was dominated by Geodesic Acoustic Modes (GAMs), and the extracted nonlinear waveforms exhibited periodic harmonic structures. Fourier analysis revealed a dominant second harmonic, while the third harmonic was unexpectedly weaker than the fourth. This nontrivial trend deviates from standard gyrokinetic predictions with a simple configuration (circular cross-section with periodic boundary condition). The results implies that symmetry breaking due to the boundary and/or plasma shape could play key roles in GAM saturation and offer guidance for refining theoretical models.

© 2025 The Japan Society of Plasma Science and Nuclear Fusion Research

Keywords: conditional average, geodesic acoustic mode, higher harmonics, nonlinear process

DOI: 10.1585/pfr.20.1203048

Transport phenomena in magnetically confined fusion plasmas are strongly influenced by the interaction between turbulence and zonal flows [1, 2]. Among these, Geodesic Acoustic Modes (GAMs), which represent the oscillatory branch of zonal flows, are known to play a crucial role in regulating turbulence levels and transport processes [3]. Understanding the physical mechanisms underlying the nonlinear saturation of GAMs is essential for controlling transport and improving plasma confinement.

Recently, harmonic generation arising from the non-linearity of GAMs has attracted considerable attention, with particular focus on the possibility that higher-order harmonics contribute to the saturation mechanism through nonlinear back-reaction [4]. However, the consistency and discrepancies of these nonlinear structures among experiments, theoretical models, and simulations have not been fully clarified.

In this study, we applied the conditional averaging technique to Heavy Ion Beam Probe (HIBP) data obtained from L-mode plasmas in the JFT-2M tokamak [5] to extract nonlinear waveforms associated with GAMs. We then compared the experimental results with those from gyrokinetic simulations performed using the GyroKinetic Vlasov (GKV) code under similar plasma conditions, in order to evaluate the consistency of harmonic structures observed in GAMs.

Electrostatic potential fluctuations were measured using the HIBP diagnostic on the JFT-2M tokamak. The target plasma conditions were as follows: toroidal magnetic field B = 1.2 T, plasma current Ip = 190 kA, neutral beam injection (NBI) heating power $P_{\scriptscriptstyle NB}$ = 750 kW, line-averaged electron density

In addition, to investigate the nonlinear behavior of GAMs, we conducted numerical simulations of electrostatic potentials using the GKV code [8]. The simulation parameters were chosen to reflect the experimental conditions of JFT-2M, and included the following values: reference ion temperature $T_{\rm ref}=1.7$ keV, normalized collision frequency $\nu=1.0$, temperature gradient $R_{\rm ax}/L_{\rm Ts}=6.92$, and density gradient $R_{\rm ax}/L_{\rm ns}=2.22$. Here, the subscript "ref" denotes the reference scale used in the GKV code. The GAM frequency obtained from the GKV simulation showed relatively good agreement with the experimental value. However, as discussed later, notable discrepancies were observed in the harmonic components of the nonlinear waveform.

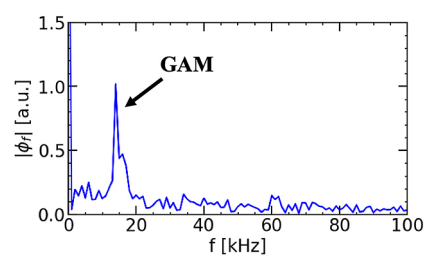


Fig. 1. Frequency spectrum of the electrostatic potential in JFT-2M.

 $[\]langle n_e \rangle = 1.1 \times 10^{19} \text{ m}^{-3}$, and safety factor $q_{95} = 2.9$. Figure 1 shows the frequency spectrum of the electrostatic potential. The radial position where the GAM amplitude reaches its maximum is analyzed. The GAM frequency approximately follows the theoretical expression [6, 7], and is evaluated to be around $f_{GAM} \approx 15 \text{ kHz}$ in this study. Here, the frequency response of the diagnostic system is considered to be sufficient [5].

 $[*]Corresponding\ author's\ e-mail:\ sasaki.makoto@nihon-u.ac.jp$

In this study, we employed a statistical technique known as conditional averaging to extract nonlinear waveforms associated with GAMs [9–11]. Originally developed for the analysis of periodic biological signals, this method enables the statistical extraction of recurring structures (templates) embedded in quasi-periodic signals, based on phase-aligned triggering events.

First, an initial template waveform $x_{j=0}(t')$ is defined, where $t' \in (-T/2, T/2)$ represents the local time within one GAM period, and the subscript j indicates the iteration number. In this study, a simple sine wave is used as the initial template. For a given measured signal y(t), the correlation function $C_j(t)$ between the signal and the template is defined as follows:

$$C_{j}(t) = \int_{-\frac{T}{2}}^{\frac{T}{2}} \frac{1}{\sigma_{\nu}(t)\sigma_{x}} (y(t-t') - \overline{y}(t))(x_{j}(t') - \overline{x_{j}})dt'.$$
 (1)

Here, $\sigma_y(t)$ and σ_x denote the standard deviations of y(t) and $x_j(t')$, respectively. From the computed correlation function $C_j(t)$, time points with high correlation values are selected as triggers. For each identified trigger time, a window of the signal y(t) is extracted over one period T, matching the length of the template. These segments are then averaged to obtain an updated template, given by the following expression:

$$x_{j+1}(t') = \sum_{i} \frac{y(t - t_{peak,j}(i))}{n}.$$
 (2)

Here, n represents the total number of triggers. The above procedure is repeated iteratively until the template converges, resulting in a statistically reliable nonlinear waveform $x_{\infty}(t')$.

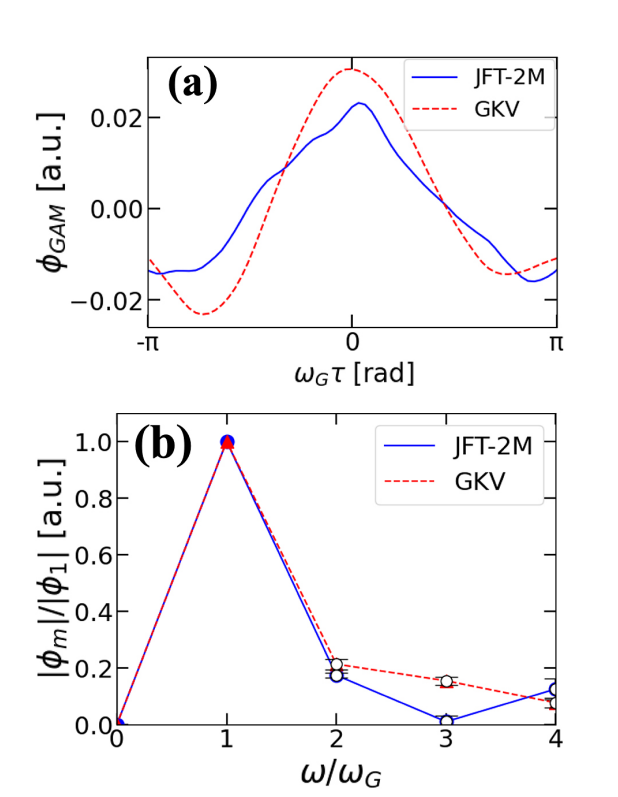


Fig. 2. (a) Overplot of converged nonlinear waveforms (templates) from JFT-2M and GKV, (b) Harmonic amplitudes.

Conditional averaging was applied to the HIBP timeseries data obtained in JFT-2M to extract statistically reliable nonlinear waveforms over the GAM period. The resulting waveform is shown in Fig. 2(a). In L-mode plasmas, GAMs are dominant and exhibit strong interactions with turbulence. The nonlinear nature of GAMs is theoretically predicted to lead to harmonic generation [3], and this behavior was also confirmed in the present study.

Fourier analysis was performed on the extracted waveform, and each harmonic component was evaluated using the following expression:

$$|\phi_m| = |\frac{1}{T} \int_0^T \tilde{\phi} e^{im\omega_G t} dt|. \tag{3}$$

Here, T denotes the GAM period, m is the harmonic number, and $\tilde{\phi}$ is the normalized nonlinear waveform. As shown in Fig. 2(b), the JFT-2M experiment revealed a prominent second harmonic (m=2), along with a distinctive trend where $|\phi_4|/|\phi_3| > 1$. This indicates a non-trivial structure in which the fourth harmonic is stronger than the third, suggesting the presence of symmetry breaking in nonlinear harmonic generation. A similar analysis was applied to the GKV simulation results. The extracted nonlinear waveform is shown in Fig. 2(a), and the corresponding harmonic amplitudes are displayed in Fig. 2(b). In contrast to the experiment, the GKV simulation showed a monotonic decrease in harmonic strength with increasing m, with the second harmonic being dominant, while no clear peaks were observed at the third or fourth harmonic. Figure 3 shows the convergence of harmonic amplitudes

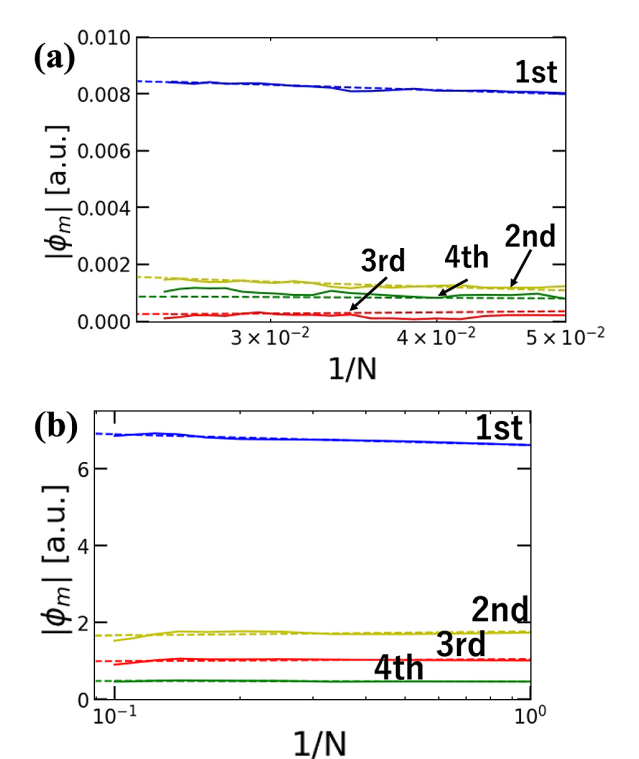


Fig. 3. Convergence of conditional-averaged harmonic amplitudes increassing ensemble size (a) JFT-2M, (b) GKV. Solid and dashed lines represent the analysis results and its linear fitting, respectively.

obtained via conditional averaging as the ensemble size, N, increases. In Figs. 3(a) and (b), which correspond to those with the experiment and GKV simulations, respectively, the good convergence can be seen in both cases. This comparison reveals that gyrokinetic models like GKV, which assume circular plasmas in periodic boundary conditions, have difficulty reproducing the higher-order harmonics observed in the experiment. In particular, the suppression of the third harmonic and the relative enhancement of the fourth suggest that asymmetries introduced by boundary and/or plasma shape may play a significant role [12, 13].

In this study, we applied the conditional averaging technique to HIBP measurements in the JFT-2M tokamak to extract statistically reliable nonlinear waveforms of GAMs. The harmonic structure obtained from these waveforms revealed a nontrivial feature—namely, the fourth harmonic being stronger than the third—which deviates from gyrokinetic predictions with periodic boundary. These findings suggest that standard models assuming idealized circular plasmas with periodic boundaries may overlook essential aspects of GAM dynamics.

The authors would like to thank Dr. K. Kamiya, and Prof.

T. Ido for fruitful discussions and valuable input. This work was partly supported by a Grant-in Aid for Scientific Research (KAKENHI) (JP21K03509, JP24K06997, JP25K00986), the collaboration programs of NIFS (NIFS24KIPS005, NIFS25KISS041), that of RIAM Kyushu University (2024S2-CD-2, 2025S2-CD-3), and OML Project by the National Institutes of Natural Sciences (NINS program No. OML012511).

- [1] W. Horton, Rev. Mod. Phys. 71, 735 (1999).
- [2] P.H. Diamond et al., Plasma Phys. Control. Fusion 47, R35 (2005).
- [3] A. Fujisawa, Nucl. Fusion 49, 013001 (2009).
- [4] M. Sasaki et al., Phys. Plasmas 16, 022306 (2009).
- [5] T. Kobayashi et al., Phys. Rev. Lett. 120, 045002 (2018).
- [6] N. Winsor et al., Phys. Fluids 11, 2448 (1968).
- [7] T. Ido et al., Plasma Phys. Control. Fusion 48, S41 (2006).
- [8] T.H. Watanabe et al., Phys. Rev. Lett. 100, 195002 (2008).
- [9] Y. Kawachi et al., Plasma Fusion Res. 14, 1402090 (2019).
- [10] S. Inagaki et al., Plasma Fusion Res. 9, 1201016 (2014).
- [11] F. Kin et al., Plasma Fusion Res. 14, 1402114 (2019).
- [12] M. Sasaki et al., Nucl. Fusion 52, 02300 (2012).
- [13] Z. Gao et al., Phys. Plasmas 15, 074502 (2008).